Onset of stimulated Raman scattering of a laser in a plasma in the presence of hot drifting electrons

D. N. Gupta, Pinki Yadav, D. G. Jang, M. S. Hur, H. Suk, and K. Avinash

Citation: Physics of Plasmas **22**, 052101 (2015); doi: 10.1063/1.4919626
View online: http://dx.doi.org/10.1063/1.4919626
View Table of Contents: http://scitation.aip.org/content/aip/journal/pop/22/5?ver=pdfcov
Published by the AIP Publishing

Onset of stimulated Raman scattering of a laser in a plasma in the presence of hot drifting electrons

D. N. Gupta,[1,a)] Pinki Yadav,[1] D. G. Jang,[2] M. S. Hur,[3] H. Suk,[2] and K. Avinash[1]
[1]*Department of Physics and Astrophysics, University of Delhi, Delhi 110 007, India*
[2]*Department of Physics and Photon Science, Gwangju Institute of Science and Technology, Gwangju 500 712, South Korea*
[3]*School of Natural Science, Ulsan National Institute of Science and Technology, Ulsan 689 798, South Korea*

(Received 30 January 2015; accepted 21 April 2015; published online 4 May 2015)

Stimulated Raman scattering of a laser in plasmas with energetic drifting electrons was investigated by analyzing the growth of interacting waves during the Raman scattering process. The Langmuir wave and scattered electromagnetic sideband wave grow initially and are dampened after attaining a maximum level that indicates a periodic exchange of energy between the pump wave and the daughter waves. The presence of energetic drifting electrons in the laser-produced plasma influences the stimulated Raman scattering process. The plasma wave generated by Raman scattering may be influenced by the energetic electrons, which enhance the growth rate of the instability. Our results show that the presence of energetic (hot) drifting electrons in a plasma has an important effect on the evolution of the interacting waves. This phenomenon is modeled via two-dimensional particle-in-cell simulations of the propagation and interaction of the laser under Raman instability. © *2015 AIP Publishing LLC*. [http://dx.doi.org/10.1063/1.4919626]

I. INTRODUCTION

Stimulated Raman scattering (SRS) of an electromagnetic wave in plasma has potential research interest because of its importance for large-amplitude plasma wave generation and corresponding electron acceleration.[1–8] In SRS, the laser wave decays into a scattered light wave and an electron plasma wave. As time passes, the plasma wave amplitude increases sufficiently to accelerate electrons to a high velocity, generating high-energy electrons. This process is most efficient when operated near a density of $n_{cr}/4$, where n_{cr} is the critical plasma density. About half of the energy of the laser light can usually be converted into high-energy electrons, as has already been observed in some experiments.[9,10] SRS may be crucial in the inertial confinement fusion process, as the scattered electromagnetic wave decreases the laser-plasma coupling and can affect the irradiation symmetry. In addition, the plasma waves can accelerate the electrons, which can heat the fusion fuel.[11,12] In a low-density plasma, forward Raman scattering is a more relevant process.[13–15] It gives rise to a high-amplitude, high-phase-velocity plasma wave that can accelerate the electrons to a very high energy. The forward Raman instability for a laser having a finite spot size may couple with the self-focusing and can produce a plasma wave of very high amplitude.[16,17]

In the field of laser-plasma interactions, hot energetic electrons have long been a concern of researches.[18–21] In common plasmas, these energetic electrons are generated by the damping of plasma waves excited by a laser. Most laser-driven fusion processes exhibit these laser-heated energetic drifting electrons as a pre-heater that pre-heats the target and affects the fuel compression.[22–24] Laser-driven electron acceleration was first observed in a laser interaction process, and now there is considerable research into high-gradient (compact) electron accelerators based on laser-plasma interactions.[25–28] These applications, however, usually apply to low-density plasmas to achieve higher electron energy gains, and the density of the accelerated electrons is controlled by the plasma density. On the other hand, a fast ignition fusion scheme requires energetic (kilojoule) electron beams that are monoenergetic. Both the high-density of the fusion target and the required high density of the (monoenergetic) electron beams require laser-plasma interactions at the critical plasma density so that the energetic electrons can be efficiently propagated into a solid target.[29,30]

We explore the SRS of a laser including the effect of energetic (hot) electrons generated during laser-plasma interactions. During laser beam propagation inside hohlraums, hot electrons can be generated by laser-plasma instabilities. We consider two types of plasma electrons of different temperatures, T_e (non-drifting) and T_d (drifting). An electromagnetic pump wave excites a Langmuir wave and an electromagnetic sideband wave. The density perturbation associated with the Langmuir wave is coupled with the electron quiver motion to produce a nonlinear current driving the sideband. Then the pump and sideband waves exert a ponderomotive force on electrons to drive the Langmuir wave even more strongly. The inclusion of energetic drifting electrons affects the growth rate of an instability. We estimate the growth rate of SRS by including the role of hot electrons and study the behavior of the interacting waves using a two-dimensional particle-in-cell (2D-PIC) computer simulation code. The numerical and simulation results are then discussed, and finally the conclusion is presented.

[a)]E-mail: dngupta@physics.du.ac.in

II. THEORETICAL MODEL

Consider a laser propagating in a plasma with two components of electrons, a non-drifting component with electron density n_0 and a drifting component with electron density n_{0d} and drift velocity $v_d\hat{z}$. The temperatures of the non-drifting and drifting electrons are T_e and T_d, respectively. The laser has an electric field

$$\vec{E}_0 = \hat{x}A_0 \exp[-i(\omega_0 t - k_0 z)]. \tag{1}$$

The response of electrons to electromagnetic fields is governed by the equation of motion and the equation of continuity. These equations are solved in conjunction with Maxwell's equations. The response of ions can be neglected as it is smaller than that of electrons by the mass ratio m/m_i, where m and m_i are the masses of an electron and an ion in the plasma, respectively.

In the SRS process, an electromagnetic pump wave $(\omega_0, \vec{k}_0)$ couples with an electrostatic perturbation $\phi = \Phi \exp[-i(\omega t - kz)]$ and generates a scattered electromagnetic sideband $\vec{E}_1 = \hat{x}A_1 \exp[-i(\omega_1 t - k_1 z)]$. The phase-matching conditions for the process can be written as $\omega_1 = \omega - \omega_0$, $\vec{k}_1 = \vec{k} - \vec{k}_0$. Using the perturbation theory, the oscillatory velocities of non-drifting electrons imparted by the interacting waves are $\vec{v}_0 = e\vec{E}_0/mi\omega_0$, $\vec{v}_1 = e\vec{E}_1/mi\omega_1$, and $\vec{v} = e\vec{E}/mi\omega$, where $\vec{E} = -\nabla\phi$ and $-e$ is the electron charge. The pump and sideband waves exert a ponderomotive force on the electrons at $(\omega, \vec{k})$, $\vec{F}_p = e\nabla\phi_p$, where $\phi_p = -(m/2e)\vec{v}_0\vec{v}_1$. The electron density perturbation at $(\omega, \vec{k})$ due to ϕ and ϕ_p is

$$n_e = \frac{k^2}{4\pi e}\chi_e(\phi + \phi_p), \tag{2}$$

where

$$\chi_e = \frac{2\omega_p^2}{k^2 v_{th}^2}\left[1 + \frac{\omega}{kv_{th}}Z\left(\frac{\omega}{kv_{th}}\right)\right]. \tag{3}$$

Here, the plasma dispersion function is $Z = 1/\pi\int_{-\infty}^{\infty} e^{-x^2}/(x-t)dx$, the electron plasma frequency is $\omega_p = (4\pi n_0 e^2/m)^{1/2}$, and the electron thermal speed can be given by $v_{th} = (2T_e/m)^{1/2}$. Similarly, we can write the response of drifting electrons as $n_{ed} = (k^2/4\pi e)\chi_{ed}(\phi + \phi_p)$, where

$$\chi_{ed} = \frac{2\omega_{pd}^2}{k^2 v_{thd}^2}\frac{1}{(1 - \omega v_d/kc^2)}\left[1 + \frac{\omega - kv_d}{(1 - \omega v_d/kc^2)kv_{thd}} \times Z\left(\frac{\omega - kv_d}{(1 - \omega v_d/kc^2)kv_{thd}}\right)\right]. \tag{4}$$

Here, $\omega_{pd} = (4\pi n_{0d}e^2/m)^{1/2}$ and $v_{thd} = (2T_d/m)^{1/2}$. Using these expressions in Poisson's equation, we obtain

$$\varepsilon\varphi = -(\chi_e + \chi_{ed})\phi_p, \tag{5}$$

where $\varepsilon = 1 + \chi_e + \chi_{ed}$.

In the absence of the pump ($\varepsilon = 0$), the modified dispersion relation of the plasma wave can be obtained as $1 + \chi_e + \chi_{ed} \approx 0$, i.e., $\omega^2 = \omega_p'^2 + (3/2)k^2 v_{th}^2$, where $\omega_p'^2 = \omega_p^2[1 + \omega_{pd}^2 v_{th}^2/\omega_p^2 v_{thd}^2(1 - \omega v_d/kc^2)]$ is the modified electron plasma frequency. The last term in this expression shows the impact of hot drifting electrons on the Langmuir wave. In the absence of hot electrons ($n_{0d} \approx 0$), the second term in the expression of the modified plasma frequency becomes zero and the dispersion relation of the plasma wave will be governed as usual by $\omega^2 = \omega_p^2 + (3/2)k^2 v_{th}^2$. Thus, the drifting electrons modify the dispersion relation of the plasma wave, and consequently, the growth rate of the SRS instability is affected.

Both the drifting and non-drifting electron density perturbations at $(\omega, \vec{k})$ couple with the oscillatory velocity because the pump produces a nonlinear current at $(\omega_1, \vec{k}_1)$, $\vec{J}_1^{NL} = -(n_e + n_{ed})e\vec{v}_0^*/2$. Following the standard method,[31] the dispersion relation of the sideband electromagnetic wave can be written as

$$\varepsilon_1\vec{E}_1 = -4\pi i\omega_1\vec{J}_1^{NL}, \tag{6}$$

where $\varepsilon_1 = \omega_1^2 - \omega_p^2 - k_1^2c^2$. Using Eqs. (5) and (6), we obtain the nonlinear dispersion relation of SRS

$$\varepsilon\varepsilon_1 = \frac{k^2|v_0|^2}{4}(\chi_e + \chi_{ed}). \tag{7}$$

In the absence of the pump, ($\vec{v}_0 = 0$), the factor on the right-hand side is equal to zero, yielding the dispersion

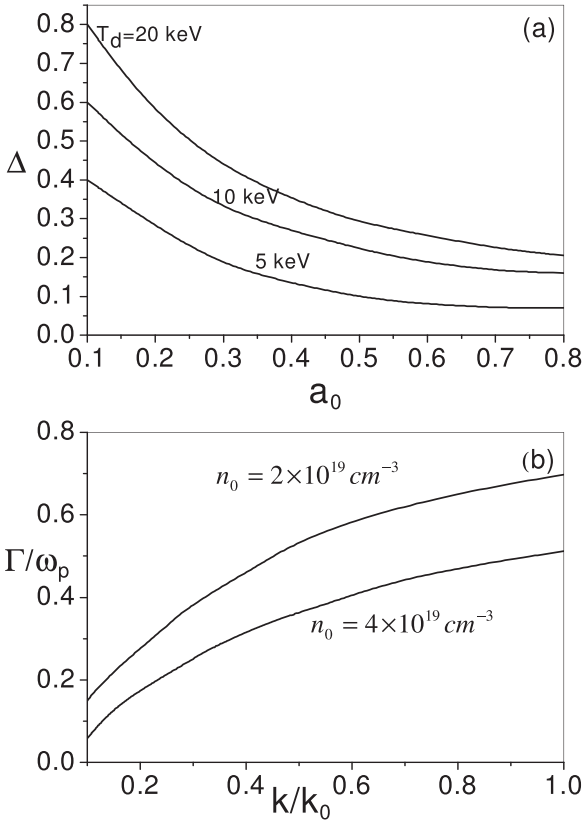

FIG. 1. (a) Variation in the relative growth difference (Δ) versus the laser intensity amplitude (a_0) for different drift electron energies ($T_d = 5$, 10, and 20 keV). The other numerical parameters are $\lambda_0 = 1.06\ \mu$m, $n_0 = 2\times10^{19}\,\text{cm}^{-3}$, $T_e = 400$ eV, and $n_{0d} = 0.1\ n_0$. (b) Variation in the normalized growth rate of SRS instability (Γ/ω_0) as a function of the normalized wave number of the electrostatic mode (k/k_0) for plasma densities of $n_0 = 2\times10^{19}\,\text{cm}^{-3}$ and $n_0 = 4\times10^{19}\,cm^{-3}$ with $T_d = 10$ keV and $a_0 = 0.5$.

relations of the Langmuir mode $(\varepsilon = 0)$ and the electromagnetic sideband wave $(\varepsilon_1 = 0)$. In a resonant decay process (when $\vec{v}_0 \neq 0$), we write $\omega = \omega_r + i\Gamma$ and $\omega_1 = \omega_{1r} + i\Gamma$, which are the roots of $\varepsilon = 0$ and $\varepsilon_1 = 0$, respectively. Now we expand ε and ε_1 around ω and ω_1, respectively, and use the Taylor expansion. Then Eq. (7) gives the growth rate of SRS as $\Gamma = \{0.44a_0^2k^2c^2/(\omega - \omega_0)\}\mathrm{Im}(\chi_e + \chi_{ed}/\varepsilon)$, where $a_0 = eE_0/mc\omega_0$ is the normalized laser amplitude. The dispersion relation of SRS can be found by taking $\chi_{ed} = 0$ in Eq. (7); consequently, the growth rate $(\Gamma_0 = 0)$ of SRS in the absence of energetic electrons can be estimated. We define $\Delta = (\Gamma_0 - \Gamma)/\Gamma_0$ as the relative growth suppression due to the energetic electrons. Fig. 1(a) shows the variation in the relative growth difference (Δ) versus the laser intensity amplitude (a_0) for different drift electron energies $(T_d = 5,\ 10,$ and 20 keV). The other numerical parameters are considered as follows: a Nd:glass laser of wavelength 1.06 μm, a hydrogen plasma density of $n_0 = 2 \times 10^{19}\,\mathrm{cm}^{-3}$, and a plasma electron temperature of $T_e = 400$ eV. For this study, we consider the energetic electron density $n_{0d} = 0.1\ n_0$.

The growth of the SRS instability decreases with increasing laser intensity amplitude, indicating greater suppression of instability growth at a higher laser-intensity. The phase velocity of the plasma wave that resonantly interacts with the drift electrons increases with increasing laser intensity and hence; reduces the growth rate of the instability. The drift electron energy plays a crucial role in the evolution of the instability growth as can be observed from Fig. 1(a). For higher-energy drift electrons, the plasma wave has a weak damping effect on the electrons. As a result, the growth rate of the SRS instability is enhanced significantly. It is observed that the growth of the instability is affected sufficiently by the laser intensity parameter. Higher pump intensity imparts more energy to the instability. In Fig. 1(b), we plot the normalized growth rate of the SRS instability (Γ/ω_0) as a function of the normalized wave number of the electrostatic mode (k/k_0) for plasma densities of $n_0 = 2 \times 10^{19}\,\mathrm{cm}^{-3}$ and $n_0 = 4 \times 10^{19}\,\mathrm{cm}^{-3}$ with a drift electron energy of 10 keV and laser intensity parameter of $a_0 = 0.5$. Our results predict that the growth rate increases with the wave number of the space-charge mode. The background plasma plays a significant role in this process. In low-density plasma, the phase velocity of the plasma wave does not increase as compared to that in the higher- density plasma. The plasma density affects the resonant interactions between the plasma wave and the drift electrons, which influences the growth of the SRS instability. This calculation shows that the growth of the SRS instability decreases with increasing plasma density in the presence of energetic electrons.

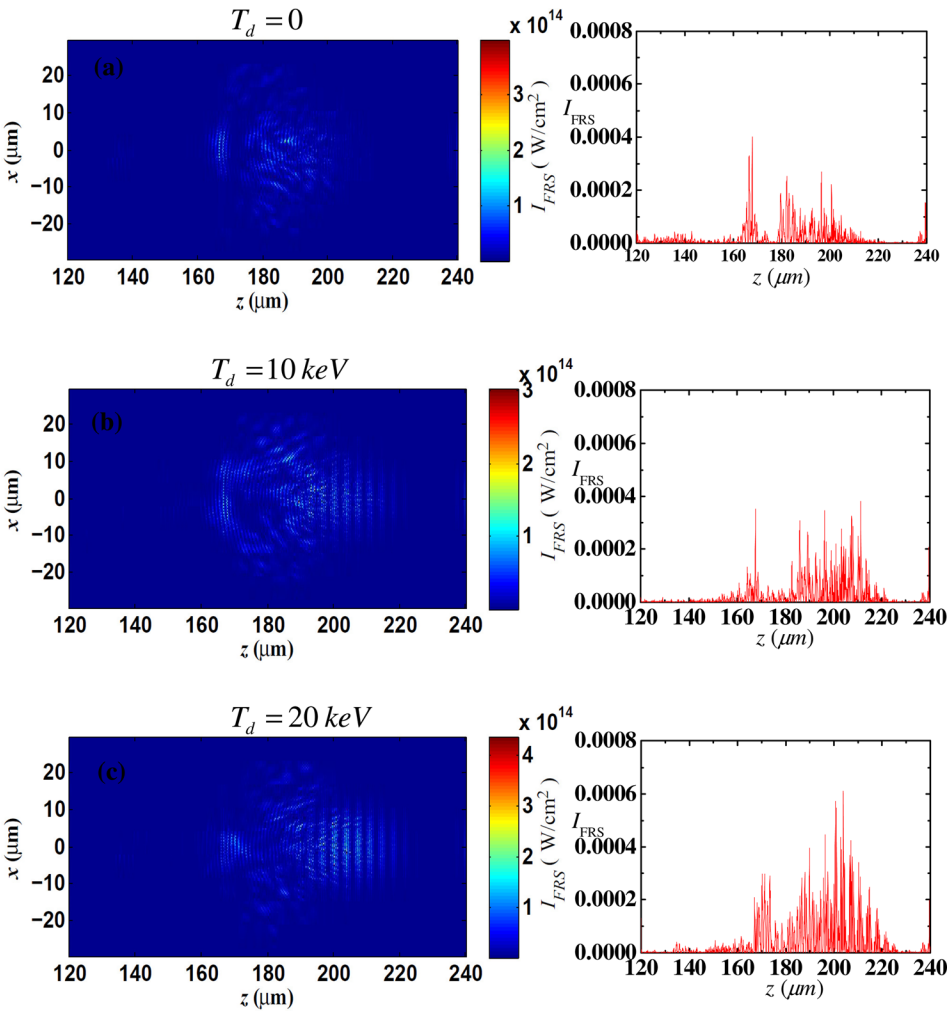

FIG. 2. Snapshots of the intensity of the FRS sideband (left-hand side) and the corresponding intensity profiles of the FRS sideband (right-hand side) at time $t = 0.8$ ps for $I_0 \approx 3.5 \times 10^{17}\,\mathrm{W/cm^2}$.

III. 2D-PIC SIMULATIONS

We perform two-dimensional simulations using a 2D-PIC code to gain insight into SRS in the presence of energetic electrons. We launch a laser pulse with a normalized intensity amplitude of $a_0 \approx 8.5 \times 10^{10} I_0^{1/2} (\mathrm{W/cm^2})\, \lambda_0\ (\mu\mathrm{m}) \approx 0.5$ (for a central wavelength of $\lambda_0 = 1.06\,\mu$m with the corresponding laser period $T_0 \approx 3.3$ fs, critical density $n_{cr} \approx 0.98 \times 10^{21}\,\mathrm{cm^{-3}}$, and laser intensity $I_0 \approx 3.5 \times 10^{17}\,\mathrm{W/cm^2}$) and focused to a spot size of $r_0 = 10\,\mu$m. The pulse has a Gaussian transverse and temporal profile with a 31.5 fs pulse duration. The laser pulse propagates along the z-direction through a plasma slab with a background density of $n_0 \approx 2 \times 10^{19}\,\mathrm{cm^{-3}}$ with a linear upward transition of 30 c/ω_p followed by a constant density over 1000 c/ω_p; then it propagates with a symmetric downward density transition of 30 c/ω_p. A simulation box with dimensions of $50 \times 200\,\mu\mathrm{m}^2$ moves at the speed of light and is resolved by 1000×200 cells. Twenty particles per cell are used for the simulations. The initial electron and ion velocities are assumed to have Maxwellian distributions with an electron temperature of 400 eV. To estimate the effect of hot electrons, the distribution of energetic (hot) electrons with temperatures of 10 and 20 keV in this plasma slab is considered for different cases of the present simulation study. Fig. 2 shows the spatial location of forward Raman scattered (FRS) light at time $t = 0.8$ ps for a laser intensity of $I_0 \approx 3.5 \times 10^{17}\,\mathrm{W/cm^2}$ and drift electron temperatures of $T_d = 0$, 10, and 20 keV.

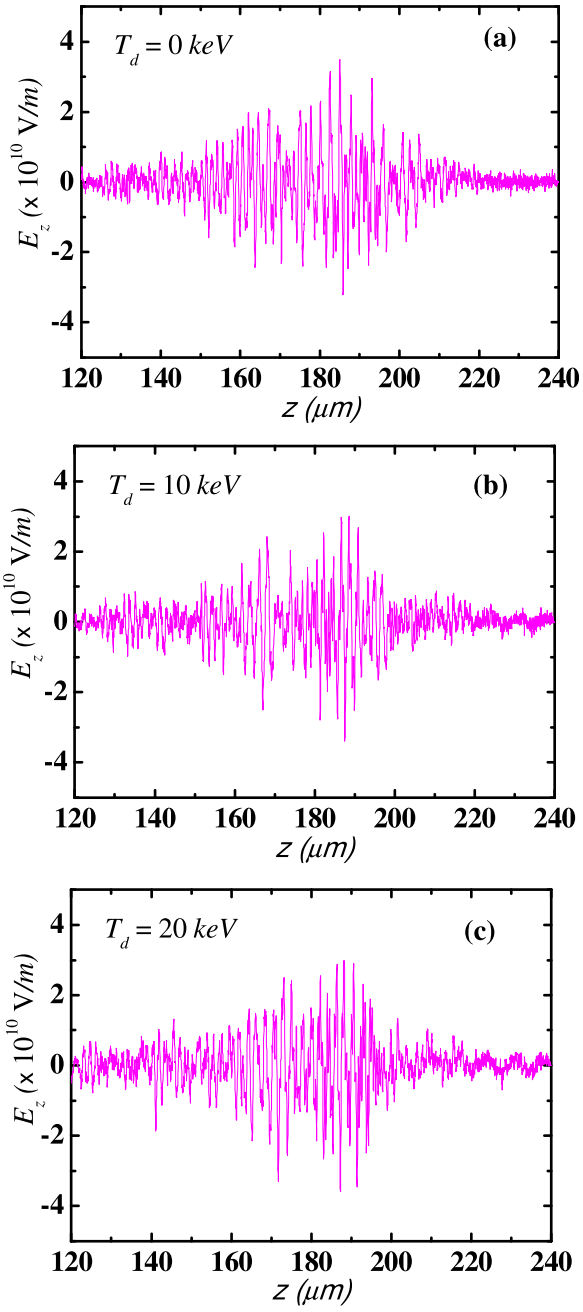

FIG. 3. Spatial dependence of the longitudinal electrostatic fields at time $t = 0.8$ ps for $I_0 \approx 3.5 \times 10^{17}\,\mathrm{W/cm^2}$ and drift electron temperatures of (a) $T_d = 0$, (b) $T_d = 10$ keV, and (c) $T_d = 20$ keV.

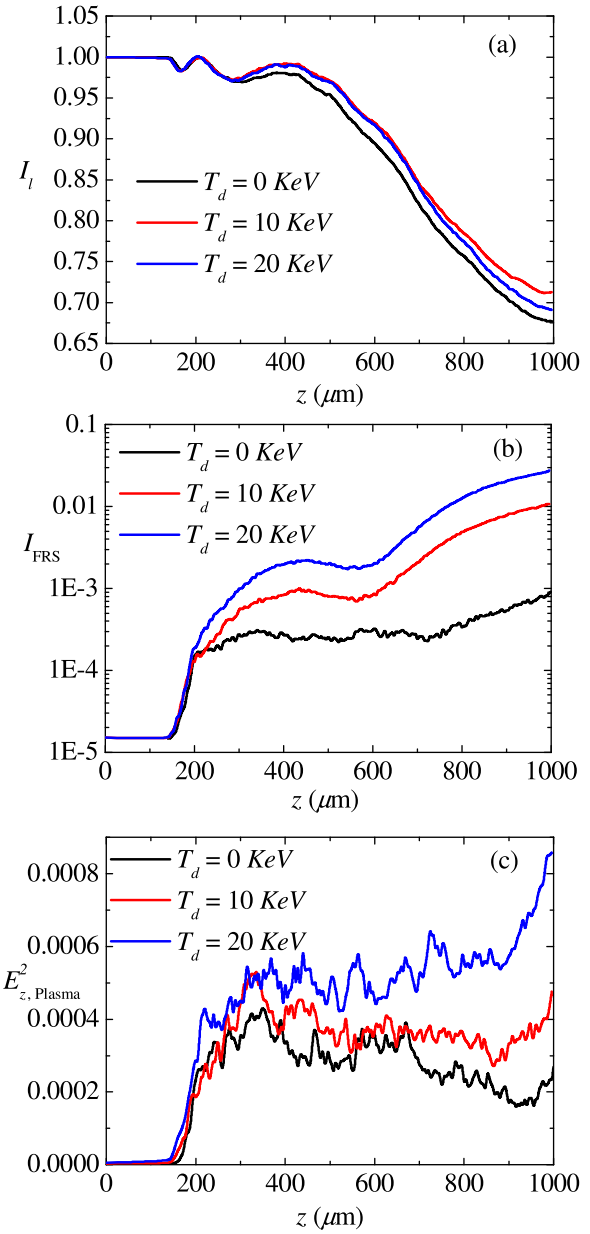

FIG. 4. Evolution of (a) pump laser intensity, (b) sideband wave intensity, and (c) plasma wave intensity with propagation distance for different drift electron energies ($T_d = 0$, 10, and 20 keV) for $a_0 = 0.5$, $\lambda_0 = 1.06\ \mu$m, and $n_0 = 2 \times 10^{19}\,\mathrm{cm^{-3}}$.

The snapshots of the spatial intensity distribution measured at time $t = 0.8$ ps show stronger FRS for higher-temperature of energetic electrons. We also examine the intensity of FRS associated with SRS to explain the interaction dynamics. The FRS spectral intensity peaks at different locations and becomes stronger at higher drift electron temperatures. The stronger FRS can thus couple to neighbors, seeding strong SRS and leading to side-scattered waves with a scattered light coherence width comparable to that of an individual sideband. Similarly, the corresponding longitudinal electrostatic fields of the plasma wave at time $t = 0.8$ ps are shown in Fig. 3. The electron plasma wave starts to grow, when the fundamental wave and the sideband first meet.

To explain the interaction dynamics of the interacting waves in SRS, for a simulation in the given plasma slab at a laser intensity of $I_0 \approx 3.5 \times 10^{17}$ W/cm^2, Fig. 4(a) shows the variation in the intensity (normalized by the initial laser intensity I_0) of the pump field with the propagation distance (in μm) in the presence of drift electrons of energy $T_d = 0$ (black curve), $T_d = 10$ keV (red curve), and $T_d = 20$ keV (blue curve) for the laser intensity parameter $a_0 = 0.5$. A plasma electron density of $n_0 = 2 \times 10^{19}$ cm^{-3} is considered for this example, and the other simulation parameters are the same as those given above.

The intensity of the electromagnetic pump wave decreases, and its energy is diverted to the daughter waves; consequently, the instability grows. As the laser propagates further in the plasma, the growth of the instability is enhanced by the energetic drift electrons; hence, the pump wave amplitude diminishes. As the instability grows, the amplitudes of the daughter waves (electromagnetic sideband and plasma waves) increase owing to energy transfer among the interacting waves. This is a parametric process in which the pump wave loses energy to the daughter waves owing to the seeding effect of the instability. Figs. 4(b) and 4(c) also show the intensity amplitude variations of the electromagnetic sideband and plasma wave versus the propagation distance for different drift electron energies. Initially, the amplitudes of the daughter waves increase because of the energy conservation law. As time grows, however, the plasma wave is damped by the electrons and loses some of its energy for $T_d = 0$ (black curve). Therefore, the growth of the instability decreases to a low level. From the simulation results, we can estimate the effect of energetic electrons. Hot electrons can travel deeper into the plasma and can affect the growth of SRS in fusion plasma. The results show that the energetic drifting electrons reduce the damping of the plasma wave. From these results, one may observe that drift electrons with higher energy affect the growth of the SRS instability significantly by weakening the damping of the plasma wave. The plasma wave and drift electrons interact resonantly, enhancing the growth of the instability. This process

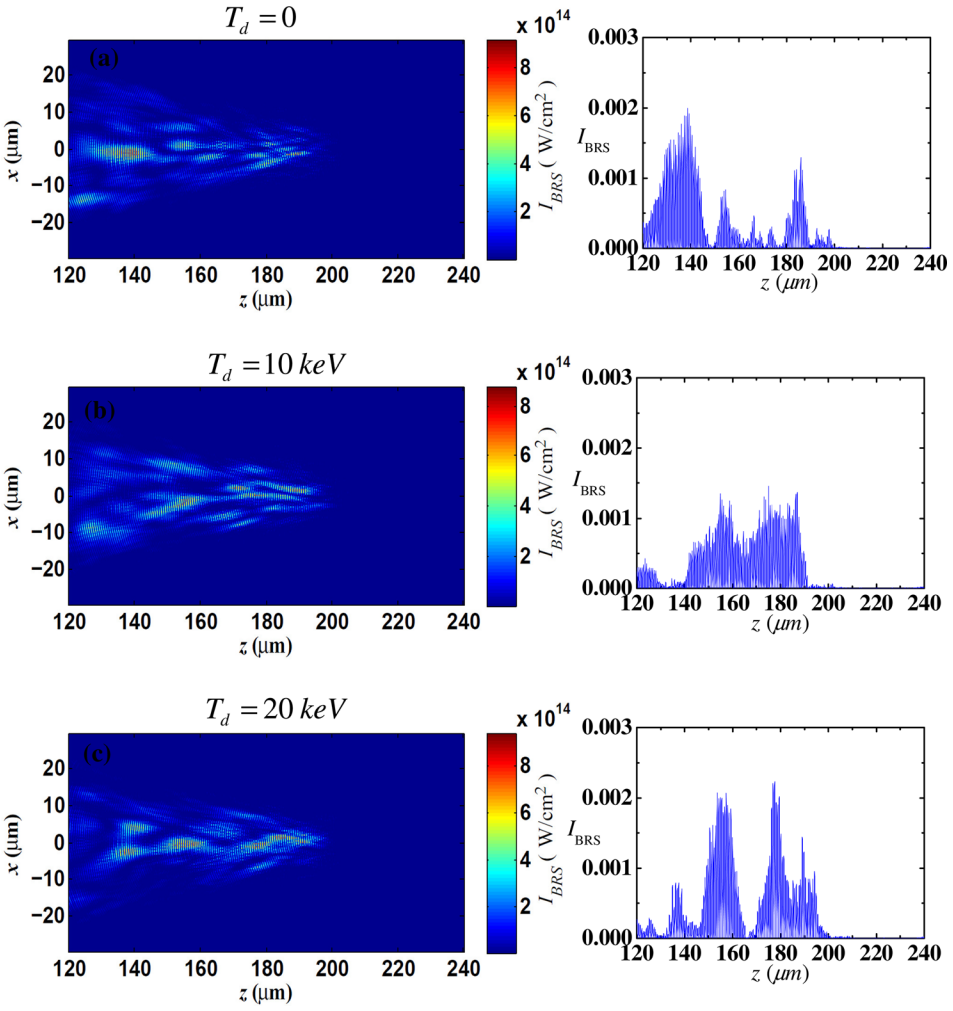

FIG. 5. Snapshots of the intensity of the Raman backward scattered sideband (left-hand side) and the corresponding intensity profile of the Raman backward scattered sideband (right-hand side) at time $t = 0.8$ ps for $I_0 \approx 3.5 \times 10^{17}$ W/cm^2.

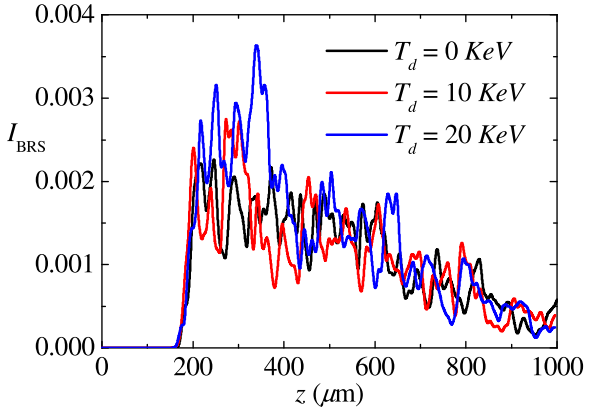

FIG. 6. Evolution of the backscattered sideband wave intensity for different drift electron energies ($T_d = 0,\ 10,$ and 20 keV) for $a_0 = 0.5$, $\lambda_0 = 1.06$ μm, and $n_0 = 2 \times 10^{19}$ cm^{-3}.

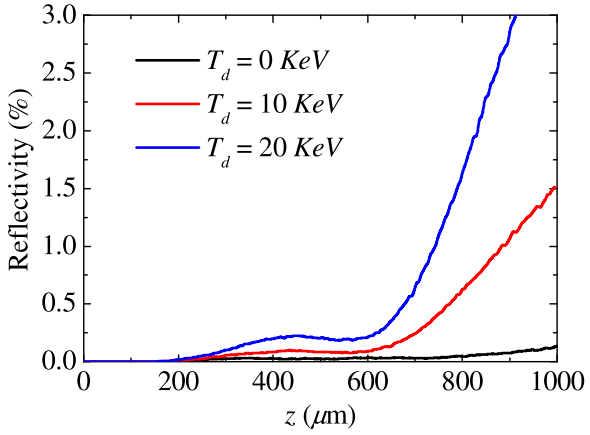

FIG. 7. SRS reflectivity (in percent) obtained from PIC simulations as a function of the interaction length for different drift electron energies ($T_d = 0,\ 10,$ and 20 keV) at time $t = 0.8$ ps for $I_0 \approx 3.5 \times 10^{17}$ W/cm^2.

is more dominant if more energetic drift electrons are present in the plasmas. The higher temperature of the drift electrons enhances the level of SRS instability growth. If the pump laser intensity increases, the plasma wave growth can become comparable to that of the sideband wave. The phase velocity of the plasma wave increases in that case, which facilitates resonant interactions between the plasma wave and drift electrons. This may be a reason to grow the plasma wave amplitude after attaining a saturation level.

So far, we have discussed the forward Raman scattering in the simulation results. However, it is worth discussing the backward SRS in underdense plasmas. The wave number matching condition for a density less than one-quarter of the critical density can be described as $\vec{k}_1 = \vec{k} \pm \vec{k}_0$, where the $\pm$ sign indicates backward or forward scattering. The theoretical explanation given in Sec. II is also validated for backward SRS. Fig. 5 shows the spatial location of backward Raman scattered (BRS) light at time $t = 0.8$ ps for a laser intensity of $I_0 \approx 3.5 \times 10^{17}$ W/cm^2 for drift electron temperatures of $T_d = 0$, 10, and 20 keV. Fig. 6 shows the intensity of the backward Raman scattered sideband versus the propagation distance for different drift electron temperatures ($T_d = 0,\ 10,$ and 20 keV). In laser-plasma interactions, backward SRS dominates forward SRS because of its larger gain, as the growth of forward SRS requires more time. Thus, the intensity of the back-scattered Raman sideband is shown to be higher in the early stage and then reduced by the significant growth of the forward-scattered Raman sideband. The energetic drifting electrons are also shown to have similar effects on the growth of the backscattered Raman sideband as in the case of forward scattering, and the backward Raman scattering is seriously affected by the presence of hot drifting electrons in fusion plasmas.

Raman reflectivity is a major issue for inertial confinement fusion. Thus, finally, it would be worth discussing the Raman reflectivity in the present case. We estimate the Raman reflectivity (R in percent) using the numerical solutions obtained from the PIC simulations. Fig. 7 shows our prediction. In a typical case, where drift electrons are not present in the plasma, the Raman reflectivity is shown to be less than 1% (black curve). However, the Raman reflectivity is greatly increased when energetic drifting electrons are present in the plasma. Although, this effect is dominant if the interaction length is sufficiently large because the large system length reduces the onset threshold and enhanced the SRS. Our results show the SRS instability with a reflectivity of $R > 1\%$ at an 8 ps interaction time owing to the stronger SRS associated with the lateral transport of hot electrons.

IV. DISCUSSION

We explored the effects of energetic drifting electrons on the SRS instability growth and consequently the temporal evolution of the interacting waves in this scenario. The PIC simulation results showed that the growth of the SRS instability was significantly affected by the presence of hot drifting electrons. The SRS growth was enhanced by the presence of drifting electrons. These drifting electrons have a dominant role in the dissipation of the plasma wave energy, which reduces the suppression of the SRS growth. Consequently, the temporal evolution of the interacting waves was also affected owing to the parametric interactions. Our finding through PIC simulation shows that the nonlinear process is crucially affected by energetic drifting electrons in the SRS. This study may be very important for understanding laser-plasma interactions when energetic (hot) drifting electrons are present with a solid target as well as for fast ignition fusion.

ACKNOWLEDGMENTS

This work was supported by the Department of Science and Technology, Government of India and the University of Delhi, India under the R&D program 2013. This research was also financially supported by the National Research Foundation of Korea (Grant Nos. NRF-2014M1A7A1A01030173 and R15-2008-006-01001-0).

[1]D. W. Forslund, J. M. Kindel, and E. L. Lindman, Phys. Fluids **18**, 1002 (1975).
[2]W. B. Mori, C. D. Decker, D. E. Hinkel, and T. Katsouleas, Phys. Rev. Lett. **72**, 1482 (1994).
[3]X. Feng and S. Lee, Appl. Phys. B **64**, 671 (1997).

[4]M. S. Hur, R. R. Lindberg, A. E. Charman, J. S. Wurtele, and H. Suk, Phys. Rev. Lett. **95**, 115003 (2005).
[5]P. K. Shukla, B. Eliasson, M. Marklund, L. Stenflo, I. Kourakis, M. Parviainen, and M. E. Dieckmann, Phys. Plasmas **13**, 053104 (2006).
[6]C. Joshi, T. Tajima, J. M. Dawson, H. A. Baldis, and N. A. Ebrahim, Phys. Rev. Lett. **47**, 1285 (1981).
[7]R. Bingham, J. T. Mendonça, and P. K. Shukla, Plasma Phys. Control. Fusion **46**, R1 (2004).
[8]P. Jha, G. Raj, and A. K. Upadhyaya, IEEE Trans. Plasma Sci. **34**, 922 (2006).
[9]A. Modena, Z. Najmudin, A. E. Dangor, C. E. Clayton, K. A. Marsh, C. Joshi, V. Malka, C. B. Darrow, and C. Danson, IEEE Trans. Plasma Sci. **24**, 289 (1996).
[10]T. Matsuoka, C. McGuffey, P. G. Cummings, Y. Horovitz, F. Dollar, V. Chvykov, G. Kalintchenko, P. Rousseau, V. Yanovsky, S. S. Bulanov, A. G. R. Thomas, A. Maksimchuk, and K. Krushelnick, Phys. Rev. Lett. **105**, 034801 (2010).
[11]J. D. Lindl, P. Amendt, R. L. Berger, S. G. Giendinning, S. H. Glenzer, S. H. Haan, R. L. Kauffman, O. L. Landen, and L. J. Sutter, Phys. Plasmas **11**, 339 (2004).
[12]H. Hora, J. Badziak, M. N. Read *et al.*, Phys. Plasmas **14**, 072701 (2007).
[13]C. S. Liu and V. K. Tripathi, Phys. Plasmas **3**, 3410 (1996).
[14]D. N. Gupta, M. S. Hur, and H. Suk, J. Appl. Phys. **100**, 103101 (2006).
[15]D. F. Gordon, H. Hafizi, R. F. Hubbard, and P. Sprangle, Phys. Plasmas **9**, 1157 (2002).
[16]T. M. Antonsen, Jr. and P. Mora, Phys. Rev. Lett. **69**, 2204 (1992).
[17]J. R. Penano, B. Hafizi, P. Sprangle, R. F. Hubbard, and A. Ting, Phys. Rev. E **66**, 036402 (2002).
[18]N. A. Ebrahim, H. A. Baldis, C. Joshi, and R. Benesch, Phys. Rev. Lett. **45**, 1179 (1980).
[19]H. Hora, *Plasmas at High Temperature and Density* (Springer Heidelberg, 1991).
[20]P. M. Nilson, A. A. Solodov, J. F. Myatt *et al.*, Phys. Rev. Lett. **105**, 235001 (2010).
[21]A. Upadhyay, V. K. Tripathi, and H. C. Pant, Phys. Plasmas **9**, 1698 (2002).
[22]F. N. Beg, A. R. Bell, A. E. Dangor, C. N. Danson, A. P. Fews, M. E. Glinsky, B. A. Hammel, P. Lee, P. A. Norreys, and M. Tatarakis, Phys. Plasmas **4**, 447 (1997).
[23]A. J. Kemp, Y. Sentoku, V. Sotnikov, and S. Wilks, Phys Rev Lett. **97**, 235001 (2006).
[24]J. Davies, A. R. Bell, M. Haines, and S. Guerin, Phys. Rev. E **56**, 7193 (1997).
[25]T. Tajima and J. M. Dawson, Phys. Rev. Lett. **43**, 267 (1979).
[26]D. Umstadter, J. Kim, E. Esarey, E. Dodd, and T. Neubert, Phys. Rev. E **51**, 3484 (1995).
[27]K. Krushelnick, Z. Najmudin, S. P. D. Mangles *et al.*, Phys. Plasmas **12**, 056711 (2005).
[28]N. A. M. Hafz, T. M. Jeong, I. W. Choi *et al.*, Nat. Photonics **2**, 571 (2008).
[29]R. G. Evans, Plasma Phys. Contol. Fusion **49**, B87 (2007).
[30]C. K. Li and R. D. Petrasso, Phys. Plasmas **13**, 056314 (2006).
[31]W. L. Kruer, *The Physics of Laser Plasma Interactions* (Addison-Wesley, New York, 1988).